

DYNAMIC DRIFT MODEL FOR GPS/INS POST-PROCESSED TRAJECTORY OF FRAME CAMERA

M. Madani and I. Shkolnikov
Z/I Imaging, an Intergraph Company
Huntsville, Alabama, USA

E-mail: msmadani@ziimaging.com; ishkolnikov@ziimaging.com

KEY WORDS: Mathematical Models, Orientation, Bundle Adjustment, Direct Georeferencing, GPS, INS, Quality Control

ABSTRACT:

GPS photogrammetry has already helped to improve the accuracy/performance of the conventional aerial triangulation process. Directly derived exterior orientation parameters using combined GPS and high-performance IMU systems offer the possibility of eliminating conventional aerial triangulation in the long run. Consequently, these changes significantly impact all the steps of the data reduction and measurement processes. However, direct georeferencing method requires additional correction for medium to large scale applications. In addition to the existing GPS/INS linear shift-drift correction per strip model, a new GPS/INS error correction model is implemented in the Intergraph’s ImageStation Automatic Triangulation (ISAT) product. Our studies have shown that for many orientation datasets of frame photos, GPS/INS errors for neighbouring positions and orientations are still highly time-correlated (even after removing a linear trend) and subject to auto regression of Gauss-Markov type rather than constant linear drift. The conducted simulation studies suggest that Wiener weighted constraints for GPS/INS error drift with trend estimation by filtering random drift residuals make a better fit than a standard linear shift-drift model for the unified least-squares bundle adjustment (Integrated Sensor Orientation) of blocks of frame photos in terms of check-point discrepancies. The purpose of this paper is to describe this new GPS/INS correction model and provide some numerical results.

1. INTRODUCTION

A photogrammetric flight with global positioning system (GPS) and inertial measurement unit (IMU) on board is a common practice today. The direct georeferencing (DGR) method for orientating aerial images using the differential-GPS/INS self-calibrating post-processing solutions for exterior orientations (EO) has sufficient accuracy for mapping applications with ground sample distance of 1-2 meters and larger. In terms of uniformity of distribution of geographic reference information, GPS data are usually much better than a typical network of the field-surveyed ground control points. However, the DGR method requires additional correction for engineering-scale applications. There are numerous sources of errors in the GPS/INS-derived EO parameters that require correction from a network of ground control points, though a much sparser one than that needed for a regular photo triangulation method. To name a few, constant shift errors are due to datum shift in position of differential GPS (DGPS) master station, difference in timing between camera mid-exposure and the GPS observation time stamp, user errors like that possible in Geoid/ellipsoid vertical datum transformations, and IMU boresight calibration errors in orientation; drift errors are due to the unresolved DGPS cycle slips, ionospheric and tropospheric delay errors increasing with distance from DGPS master station, and the unmonitored GPS antenna motion with respect to the camera body frame suspended in the inertially-stabilized mount (Mostafa and Hutton, 2001). Earth curvature and unequal horizontal and vertical map scales impose additional distortion when DGR is computed in mapping coordinate systems.

1.1 The DLC Concept

The quality of the exterior orientation data becomes directly apparent when it is combined with the imaging system data. The mapping process using directly measured exterior orientation parameters is different from the traditional one. Therefore, the entire process of quality control and quality assurance (QA/QC) becomes a process of managing each step in the data acquisition and post-mission processing phases to achieve a consistent and reliable quality assessment.

A number of QA/QC methods have been designed and developed in ISAT to allow quick evaluation of the quality of the directly measured EO parameters, camera-calibrated parameters, and datum parameters for a particular application and scale (Figure 1).

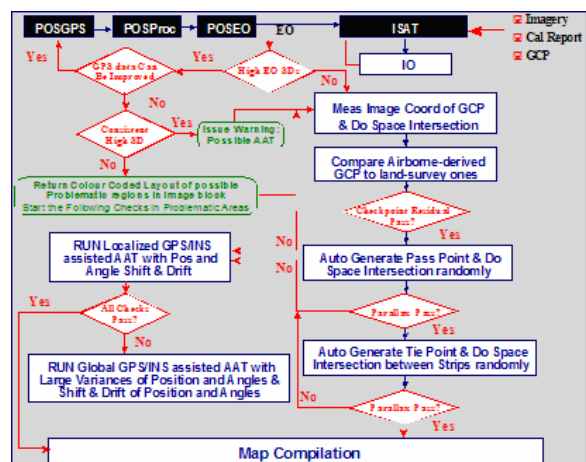


Figure 1: GPS/INS QC Tools in ISAT (DLC Concept)

Detection, Location, and Correction (DLC) is the concept behind the direct EO QA/QC process in ISAT. POS (GPS/IMU) data, project aerial imagery, and available GCP (control/check points) are simultaneously used to efficiently perform DLC. By 'detection', we mean to automatically detect whether or not there is a perfect fit (according to some predefined threshold) between the directly derived EO parameters, the images, and the available GCP. If there is no perfect fit then 'Location' is performed, where ISAT tries to identify the location and possibly the reason for erroneous EO parameters. 'Correction' is where the erroneous (inaccurate for some reason) EO parameters are corrected (Madani, and Mostafa, 2001).

EO Analysis tools and the DGR capability are used to evaluate the quality or condition of exterior orientation parameters in a project by comparing the given coordinates of control points and check points with the intersection of the rays of these points as projected on overlapping photo pairs by the EO data and by the amount of y-parallax per point and per model (see Figures 2 and 3).

Point Id	Type	Class	Photo Pair	Point Py (um)	Model Py (um)	Delta X
100002	Control	XYZ	1*2078+1*2079	213.4	233.4	-3.017
100002	Control	XYZ	1*2078+1*2079	222.7	282.2	-0.695
100002	Control	XYZ	3*2140+3*2139	142.6	142.6	0.689
100002	Control	XYZ	3*2139+3*2138	155.1	155.1	-0.154
100002	Control	XYZ	3*2138+3*2137	187.5	187.5	-0.825
100002	Control	XYZ	3*2137+3*2136	167.4	167.4	-1.312
100002	Control	XYZ	7*2129+7*2130	117.8	117.0	6.062
100002	Control	XYZ	7*2130+7*2131	118.2	118.2	5.694
100002	Control	XYZ	7*2131+7*2132	126.8	126.8	5.071
100002	Control	XYZ	7*2132+7*2133	115.9	115.9	4.182
100008	Control	XYZ	1*2082+1*2083	225.1	256.1	-0.087
100010	Control	XYZ	1*2084+1*2085	218.4	280.2	0.417
100011	Control	XYZ	1*2084+1*2085	289.4	280.2	-1.903
100014	Control	XYZ	1*2081+1*2082	302.9	302.9	-3.082

	Point Py (um)	Model Py (um)	DX (m)	DY (m)	DZ (m)
Min:	109.2	109.2	-4.413	-5.441	-2.706
Max:	373.4	337.8	6.062	6.490	3.442
Mean:	222.4	211.2	1.548	-0.184	0.525
RMS:	236.7	224.8	3.249	3.187	1.626

Figure 2: Point Parallax and Intersected Point Discrepancy

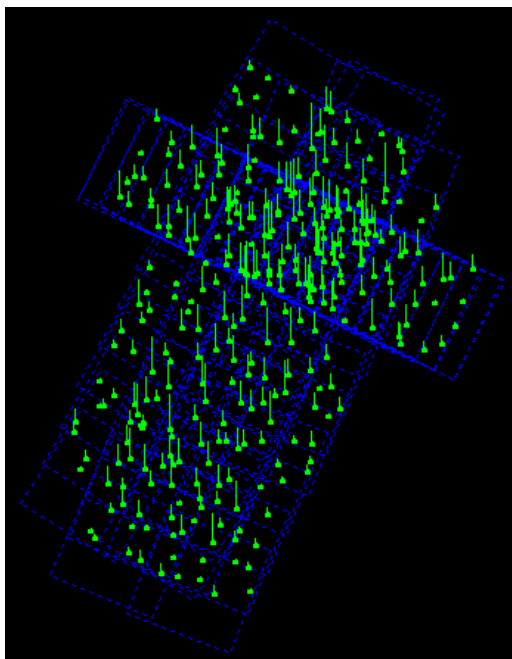


Figure 3: Display of y-parallax for Selected Models

2. GPS ERROR MODELING

A common correction method for systematic GPS/INS errors is to use piecewise polynomial splines with respect to GPS time. In many practical systems, a linear shift-drift model is used. In case of a strip of frame photos, usually one line segment per strip is employed. However, the contemporary differential-GPS/INS self-calibrating post-processing solutions do not have linear drift in time as a dominant trend neither for position, nor for orientation. Instead, these post-processed data have a common shift per block plus slow-varying, highly time-correlated drift components that do not have a general linear trend. In this case, a linear shift-drift model becomes too stiff to accommodate true GPS/INS errors even with more than one segment per strip. The result is that maximal position/attitude error may become larger than that in the original GPS/INS observation even though RMSE may be reduced, which makes the accuracy of ground-to-image transformation less uniform across the block (Madani, Shkolnikov, 2005).

There is a need for more advanced, flexible and yet simple correction models that improve a DGR corrective adjustment or an integrated sensor orientation. In the latter case, residuals on the corrected GPS/INS observations must become random to satisfy the unified least-squares optimal error distribution principle. This work is concentrated on analysis and development of shift-invariant GPS/INS drift correction models, one example of which is a first-order difference equation of the Markov system driven by Gaussian drift noise (Mikhail, 1999, Lee et al., 2000, Lee and Bethel, 2001).

Post-processed GPS errors are highly correlated in time. Therefore, it is possible to use different waveform models to correct for these errors in the least squares adjustment. The basic correction equation for each EO parameter, say X-position, is given by,

$$X_{ci} \stackrel{def}{=} X_{GPSi} + X_{\Delta i} \quad (1)$$

where X_c is the unknown camera position, X_{GPS} is the GPS position estimate of the camera (taking care of the antenna offset, if necessary), X_{Δ} is the unknown correction of the GPS position, and i is the camera station number in a strip.

For a corrective bundle adjustment with DGR, the term X_{Δ} is usually a deterministic function of time, like a piecewise linear or quadratic spline. This modelling assumption for the corrective adjustment with DGR may be sufficient for a smooth platform trajectory given at a high sampling rate, like that for satellite pushbroom scanners. However, the polynomial models are not always flexible enough to satisfy aerial platform trajectories (Mikhail, 1999, Lee et al., 2000, Lee and Bethel, 2001).

For a bundle adjustment of a block of frame photos, Eq. (1) becomes a stochastic constraint

$$X_{ci} = X_{GPSi} + a_0 + a_1 \cdot (t_i - t_0) + v_i \quad (2)$$

where residuals $\{v_i\}$ are assumed Gaussian, random and uncorrelated, a_0 and a_1 are shift and drift parameters, t_i and

t_0 are time stamps, X_{GPS_i} are GPS observations, and X_{c_i} are corrected coordinates of the camera positions, respectively. Eq. (2) is unified with collinearity and control observation equations in the least squares adjustment.

2.1 Gauss-Markov Drift Model

This model was originally employed for the aerial pushbroom scanner corrective bundle adjustment with DGR (see Lee C. and et al., 2000, Lee and Bethel, 2001) where the deterministic GPS error correction model has been replaced with the stochastic GPS error drift model, Gauss-Markov first-order autoregressive model.

The idea was to model GPS correction X_Δ drift by the following dynamics

$$\frac{dX_\Delta}{dt} = -\beta X_\Delta + n \quad (3)$$

which has a discrete time form

$$X_{\Delta_i} - (1-s)X_{\Delta_{i-1}} = v_i, \quad (4)$$

$$s = \beta \Delta t, \quad v_i = \Delta t n_i$$

where β, s are Markov continuous/discrete autocorrelation parameters, and input noise sequence $\{v_i\}$ ($n(t)$ in continuous case) is assumed Gaussian (zero-mean, known standard deviation, and uncorrelated random process). Equations of the form (4) define a stochastic constraint between adjacent unknown corrections to each GPS position. The partial derivatives of collinearity condition equations with respect to X_c are equal to that with respect to X_Δ , and unknown camera positions can be replaced by X_Δ as corresponding free parameters of the bundle adjustment due to Eq. (1). In this case there is no difference between the corrective bundle adjustment with DGR and the unified bundle adjustment with additional GPS observation equations.

It is not difficult to show that

$$E\{v_i^2\} = \sigma_{X_\Delta}^2 \left(1 + a^2 - 2a\rho_{X_\Delta}(1)\right) \quad (5)$$

where $a = 1 - s$, $\sigma_{X_\Delta}^2 = E\{X_{\Delta_i}^2\}$,

$\rho_{X_\Delta}(1) \cdot \sigma_{X_\Delta}^2 = E\{X_{\Delta_i} \cdot X_{\Delta_{i-1}}\}$, and the least squares of drift residuals

$$\min_a (E\{v_i^2\}) = \sigma_{X_\Delta}^2 \left(1 - \rho_{X_\Delta}(1)\right) \quad (6)$$

will be achieved when $a = \rho_{X_\Delta}(1)$, which is the first autocorrelation coefficient for X_Δ . The stronger is the correlation between successive GPS corrections X_Δ , the smaller is the standard deviation of input noise that drives the

GPS error drift model as compared to standard deviation of GPS error correction itself σ_{X_Δ} .

It has been reported that the Gauss-Markov first order drift model for GPS/INS error correction always gives better performance than piecewise polynomial correction models for aerial pushbroom platforms (Lee et al., 2000, Lee and Bethel, 2001).

One should notice that the optimal coefficient $a = 1 - s$ could be estimated separately from the main bundle adjustment by statistical collocation as the first autocorrelation coefficient for X_Δ estimated at a given iteration step of the system of linearized condition equations. Then at the next step, condition equations of the form (4) are written with the fixed parameter s , removing the need for any border parameters in the reduced normal equation system and leaving it as a banded-type system instead of banded-bordered.

2.2 Wiener Drift Model

While successive GPS corrections X_Δ are highly correlated for the pushbroom line-frames, they are far less correlated for successive samples of frame photos. For many practical cases, GPS error drift has a purely random drift model of the type

$$X_{\Delta_i} - X_{\Delta_{i-1}} = v_i, \quad (7)$$

where (7) could describe the relative change in the neighboring GPS corrections without extra parameters. The continuous-time equivalent of Eq. (7) defines a Wiener random process

$$\frac{dX_\Delta}{dt} = n \quad (8)$$

where $n(t)$ should be a model of a zero-centered Gaussian white noise. In a case when $\{v_i\}$ do have remaining correlation in time, filtering by statistical collocation to the main bundle adjustment may refine the model (7)

$$X_{\Delta_i} - X_{\Delta_{i-1}} = d_i + v_i, \quad (9)$$

where $\{d_i\}$ is the filtered trend surface (estimated by statistical collocation on the previous iteration step), and $\{v_i\}$ are now truly random uncorrelated drift residuals.

Finite-impulse-response (FIR) filter for trend estimation is computed by autocovariance method where the mean-removed autocorrelation of the signal (trend $\{d_i\}$) component in $\{v_i\}$ is modeled by equation $y = \exp(-p \cdot n^2)$, $n = 0, 1, 2, \dots$, where parameter p is estimated using nonlinear least-squares fit of one-sided autocorrelation $\rho_v(n)$ of zero-centered sequence $\{v_i\}$ into a set of conditions

$$F(n) = \rho_v(n) - \exp(-pn^2) \quad (10)$$

for a given number of taps $n = 0, 1, 2, \dots, N - 1$, minimizing

$$\chi^2 = \sum_{n=0}^{N-1} F^2(n) \text{ by gradient-hessian descent}$$

$$p = p^o + \partial p, \partial p = -S^{-1}D, D = \frac{\partial \chi^2}{\partial p}, S = \frac{\partial^2 \chi^2}{\partial p^2}$$

Thus, this simple method of GPS error correction with random drift model followed by collocation of FIR filtering will be adopted for testing in our case study against linear shift-drift model and will be called “dynamic drift collocation” method.

3. GPS ERROR ANALYSIS

This study is restricted to GPS error investigation as a basis for deriving and justifying GPS/INS correction models. In this section, true GPS error estimation by photogrammetric method will be performed at the sampling distances of exposure station positions of a strongly connected block of frame photos with a sufficiently redundant network of ground control points and dense population of cross-strip tie points. If there are no systematic errors in image observations and ground control points, then there is a good opportunity to have camera position estimates without systematic errors especially that correlated in flight time along a strip. Therefore, the estimate of a waveform of ideal GPS correction may be obtained as a difference between the triangulated camera positions and the GPS-estimated positions.

3.1 Test Data Description

The 1:10,000 photo scale data of the Fredrikstad, Norway test field, flown by Fotonor AS using a wide angle Leica RC30 camera equipped by an Ashtech GPS receiver and the Applanix POS/DG system, was used in this study (for detail, see Heipke, et al, 2000). This test field is about $5 \times 6 \text{ km}^2$ and has 51 well distributed signalized control points with the accuracy of about 0.01 m. The control point coordinates, raw and refined direct EO parameters were given in UTM/EuroRef80 coordinate system with ellipsoidal heights. This data set is comprised of five parallel strips and two cross strips and 13 control points (Figure 4).

Applanix POSEO data, uncorrected and corrected for boresight, computed in the phase one of the OEEPE study, along with the provided control points coordinates and the image coordinates of all 85 photos were used to investigate the different GPS/INS correction models by the ISAT bundle block adjustment program and its DLC capability for analyzing the quality of the derived EO parameters (Madani, Dörstel, Zeitler and Tang, 2001).

3.2 Numerical Results

Several bundle adjustments were performed on this block using control points, Given EO, and with different GPS/INS correction models applied. The first bundle adjustment used only control points as weighted observations. Relative bundle adjustment of this test block revealed no visible systematic errors in image residuals and no visible systematic errors in ground control/check residuals in absolute block adjustment (Figure 5). Estimated EO positions are within 7 to 11 cm. This

set of EO parameters is used as a reference for other error estimation adjustments.

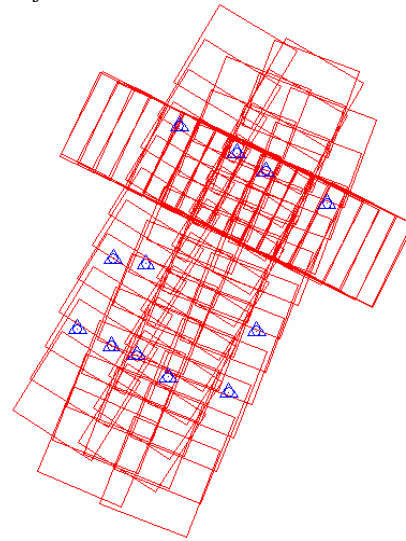


Figure 4: Calibration Flight in Southern Norway

Parameter	X/Omega	Y/Phi	Z/Kappa
RMS Control	0.0188	0.0095	0.0139
RMS Check			
RMS Limits	0.0500	0.0500	0.0500
Max Ground Residual	0.0451	0.0192	0.0293
Residual Limits	0.0500	0.0500	0.0500
Mean Std Dev Object	0.0529	0.0485	0.1080
RMS Photo Position			
RMS Photo Attitude			
Mean Std Dev Photo Position	0.1079	0.1117	0.0687
Mean Std Dev Photo Attitude	0.0032	0.0038	0.0014

Current Count		Cameras used: (1)	
Control Points Used:	13	Camera Id	Lens Dist
Check Points Used:	0	top15	Off
Photos Used:	85		
Photos Not Used:	0		
Image Points Used:	2719		

Figure 5: Absolute Bundle Adjustment Using Control Points

All adjusted object points from this reference solution were used as check points for the second bundle adjustment using control points and given GPS/INS data as weighted observations (Figure 6).

Computed camera positions are compared with the corresponding GPS values. Derived GPS errors are up to 60 cm. One can clearly see that RMS values of the check points in Z are much higher than the estimated precision in Z. This is due to the systematic distortion of the GPS observations. Analyzing these two bundle adjustments (Figures 5 and 6), one can conclude that GPS errors in Figure 6 are well above the estimated noise level due to the photogrammetric method (compare Std Devs and RMS on control/check points and EO position Std Devs). Thus, if the fit into this control network is considered as a reference one, then the GPS correction model for the additional GPS observations to be included into adjustment must absorb waveforms given in Figure 7 in order to produce a set of EO positions maximally consistent with the

block geometry enforced by this dense control network. One can clearly see that a linear shift-drift correction is a fair candidate only for X-correction waveform, while it is too rigid for the other two (Madani and Shkolnikov, 2005).

Parameter	X/Omega	Y/Phi	Z/Kappa
RMS Control	0.0171	0.0097	0.0151
RMS Check	0.0110	0.0147	0.1733
RMS Limits	0.0500	0.0500	0.0500
Max Ground Residual	0.0361	0.0159	0.0377
Residual Limits	0.0500	0.0500	0.0500
Mean Std Dev Object	0.0499	0.0458	0.0970
RMS Photo Position	0.2893	0.3134	0.5614
RMS Photo Attitude	0.0927	0.0895	0.1789
Mean Std Dev Photo Position	0.0969	0.0972	0.0577
Mean Std Dev Photo Attitude	0.0029	0.0033	0.0013

Current Count	Camera Id	Lens Distr
Control Points Used: 13	top15	Off
Check Points Used: 308		
Photos Used: 85		
Photos Not Used: 0		
Image Points Used: 2719		

Figure 6: Absolute Bundle Adjustment Using Control Points and GPS/INS data

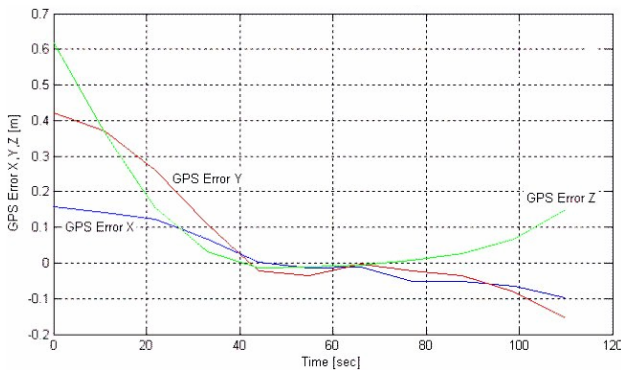


Figure 7: Estimated GPS Errors

The problem with a linear shift-drift correction here is that there are too many given GPS positions as compared to the number of control points in a typical adjustment; they tend to impose an extra residual load on controls accounting for their own errors in the unified least squares adjustment, which becomes invalid since it assumes uncorrelated errors in given EO while they indeed are highly correlated along the strip.

A difference between the reference camera positions and the GPS-estimated positions for one selected strip is shown in Figure 7. One can observe that GPS errors are highly time-correlated, and correction waveform bandwidth is much lower than the Nyquist limit set by sampling at exposure points. Normalized autocorrelations for waveforms are given in Figure 8.

GPS errors would be still highly correlated after linear trend removal even with sparse sampling at exposure stations. Derived GPS error in Z has a significantly parabolic trend. Therefore, the linear correction model cannot express this behaviour (Figure 7). More flexible correction models that

account for higher frequency changes in the EO parameters can be obtained.

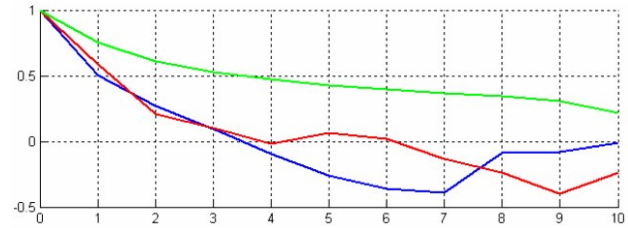


Figure 8: Normalized Autocorrelations of GPS Errors

GPS Error Drift (the first difference of GPS error) has much more random error distribution along a strip than GPS Error itself even with linear trend removed (Figure 9).

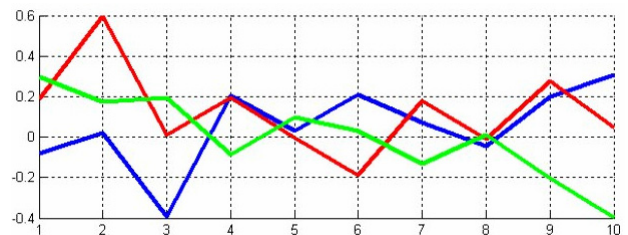


Figure 9: First Differences of GPS Errors

One can identify that the GPS error drift is correlated within a window of ± 5 photos. Thus, the idea to impose stochastic constraints on GPS error drift has two obvious merits: first, a drift constraint controls relative change in EO position from photo to photo while absolute geo-datum will be controlled entirely by ground control points (i.e., this is a shift-invariant constraint); second, GPS error drift model driven by random noise is more flexible than a piecewise constant drift model (linear shift-drift) where random noise is attributed to shift residuals.

Figures 10 and 11 present general statistics on bundle adjustment performed with linear shift-drift GPS correction model (Figure 8) and dynamic drift collocation model (Figure 11). One can observe that RMS in Z coordinate on check points has dropped 10 fold, which was expected since linear correction is a poor model for Z-error in GPS (Figure 7), while dynamic drift was able to accommodate this trend completely.

Parameter	X/Omega	Y/Phi	Z/Kappa
RMS Control	0.0186	0.0096	0.0132
RMS Check	0.0043	0.0044	0.0584
RMS Limits	0.0500	0.0500	0.0500
Max Ground Residual	0.0449	0.0185	0.0281
Residual Limits	0.0500	0.0500	0.0500
Mean Std Dev Object	0.0514	0.0472	0.1026
RMS Photo Position	0.1424	0.1292	0.1884
RMS Photo Attitude	0.0000	0.0000	0.0000
Mean Std Dev Photo Position	0.1028	0.1042	0.0637
Mean Std Dev Photo Attitude	0.0031	0.0036	0.0014

Current Count	Camera Id	Lens Distr
Control Points Used: 13	top15	Off
Check Points Used: 308		
Photos Used: 85		
Photos Not Used: 0		
Image Points Used: 2719		

Figure 10: Bundle Adjustment with GPS Linear Shift/Drift

Parameter	X/Omega	Y/Phi	Z/Kappa
RMS Control	0.0189	0.0096	0.0140
RMS Check	0.0012	0.0013	0.0057
RMS Limits	0.0500	0.0500	0.0500
Max Ground Residual	0.0457	0.0193	0.0294
Residual Limits	0.0500	0.0500	0.0500
Mean Std Dev Object	0.0512	0.0470	0.1030
RMS Photo Position	0.0829	0.0952	0.0323
RMS Photo Attitude	0.0000	0.0000	0.0000
Mean Std Dev Photo Position	0.1025	0.1043	0.0644
Mean Std Dev Photo Attitude	0.0030	0.0036	0.0014

Current Count	Camera Id	Lens Dist
Control Points Used: 13	top15	Off
Check Points Used: 308		
Photos Used: 85		
Photos Not Used: 0		
Image Points Used: 2719		

Figure 11: Bundle Adjustment with GPS Dynamic Drift

4. CONCLUSIONS

A simple method of GPS/INS error correction is developed that does not require any additional parameters in the bundle adjustment solution, which contribute to the border of otherwise banded-type matrix of the reduced normal equation system of the iterative least squares adjustment for a block of frame photos. The proposed random drift model (Wiener drift model) is placing a stochastic constraint on the relative change in GPS/INS correction (weighing relative distances between exposure points rather than absolute positions of each exposure), hence modeling the correction in a shift-invariant mode with drift dynamics given by a Wiener process. Absolute datum in this case is controlled entirely by ground control points. The trend in random drift is estimated by collocation of autocovariance finite-impulse-response filter. The proposed GPS/INS correction model is proven to be more flexible than a standard linear shift-drift model in accommodating higher frequency changes of GPS/INS error. Experiments with GPS correction by the proposed dynamic drift model have been performed on a modified version of ZI Imaging *ISAT/PhotoT* software, which is going to adopt this new method of GPS/INS correction as an option in the future commercial releases of this software.

5. REFERENCES

- Heipke, C., Jacobsen, K., Wegmann, H., Anderson, O., Nilsen, B. (2000), "Integrated Sensor Orientation – An OEEPE Test", IAPRS, Vol. XXXIII, Amsterdam, 2000.
- Lee C., Theiss H. J., Bethel J. S., and E. M. Mikhail (2000). "Rigorous mathematical modelling of airborne pushbroom imaging systems," *Photogrammetric Engineering and Remote Sensing*, vol. 66, No. 4, 2000, pp. 385-392.
- Lee C., and J. S. Bethel, "Georegistration of airborne hyperspectral image data (2001)." *IEEE Transactions on Geoscience and Remote Sensing*, vol. 39, No. 7, 2001, pp. 1347-1351.

Madani, M., Mohamed, M. (2001). "ISAT Direct Exterior Orientation QA/QC Strategy Using POS Data." OEEPE Workshop – Integrated Sensor Orientation. Hanover, Germany, September 17-18.

Madani, M., C. Dörstel, W. Zeitler and L. Tang (2001). "ZI Imaging's new automatic aerial triangulation system," *Proceedings of 2001 Annual Conference of American Society of Photogrammetry and Remote Sensing*, (CD ROM).

Madani, M., Shkolnikov, I. (2005). "Photogrammetric Correction of GPS/INS Post-Processed Trajectory of the Frame Camera Platform Using Ground Control." ASPRS Conference Proceedings, Baltimore, Maryland, March 7-11, 2005.

Mikhail, E. M. (1999). "Is photogrammetry still relevant," *Photogrammetric Engineering and Remote Sensing*, vol. 65, No. 7, 1999, pp. 740-751.

Mostafa, M.M.R., Hutton, J. (2001). "Direct Positioning and Orientation Systems: How Do They Work? What is The Attainable Accuracy?" ASPRS Annual Conference, St. Louis, MO, USA, April 23 – 27.